Robust Model Matching for Geometric Fault Detection Filters: A Commercial Aircraft Example ⋆

Bálint Vanek * **Peter Seiler** ** **József Bokor** * **Gary J. Balas** **

* *Systems and Control Laboratory, Computer and Automation Research Institute, Hungarian Academy of Sciences (vanek@sztaki.hu).*
** *Aerospace and Engineering Mechanics Department, University of Minnesota (seiler@aem.umn.edu).*

Abstract: Geometric fault detection and isolation filters are known for having excellent fault isolation, fault reconstruction and sensitivity properties under small modeling uncertainty and noise. However they are assumed to be sensitive to model uncertainty and noise. This paper proposes a method to incorporate model uncertainty into the design. First, a geometric filter is designed on the nominal plant. Next a robust model matching problem is solved to design a filter that robustly matches the performance of the geometric filter over the set of uncertain plants. Several existing methods for robust filter synthesis are described to solve the robust model matching problem. It is then shown that the robust model matching problem has an interesting self-optimality property for multiplicative input uncertainty sets. Finally, an aircraft dynamics example is presented to detect and isolate aileron actuator faults to asses the performance of the geometric filter.

1. INTRODUCTION

Modern fly-by-wire aircraft flight control systems are becoming more complex with many actuators controlling several aerodynamic surfaces. While performance goals, like aerodynamic drag minimization and structural load suppression are becoming more and more important flight must be kept at the same highest safety level. In parallel, there is a clear trend towards the All-Electric Aircraft. Recently, Airbus introduced on the A380 a new hydraulics layout [Van den Bossche, 2006], where the three Hydraulics circuitry is replaced by a two Hydraulics plus two Electric layout, which saves one ton mass for the aircraft. Each primary surface has a single hydraulically powered actuator and electrically powered back-up with the exception of the outer aileron, which uses the two hydraulic systems together. Consequently, the trends of complexity and more-electric architectures, like Electromechanical Actuators (EMA) with more fault sources, raise the importance of availability, reliability and operating safety. For safety critical systems, like aircraft, the consequence of faults in the control system hardware and software can be extremely serious in terms of human mortality and economical impact. This is the reason why all aircraft manufacturers are compliant with stringent safety regulations of FAA, EASA and other aviation authorities. However, there is a growing need for on-line supervision and fault diagnosis to satisfy the newer societal imperatives towards an environmentally-friendlier aircraft with still the highest level of safety and reliability. The traditional approach to fault diagnosis in the wider application context is based on hardware redundancy methods which use multiple sensors, actuators computers and software to measure and control a particular variable [Goupil, 2009a]. Based on the mathematical model of the plant, analytical relation between different sensor outputs can be used to generate residual signals. There is a growing interest in methods which do not require additional hardware redundancy, and only rely on the ever increasing level of computational power onboard the aircraft. In analytical redundancy schemes, the resulting difference generated from the consistency checking of different variables is called as a residual signal. The basis for residual generation is analytical redundancy, which according to Chow and Willsky [1984] takes two forms: 1) direct redundancy-the relationship among instantaneous outputs of sensors; and 2) temporal redundancy-the relationship among the histories of sensor outputs and actuator inputs. It is based on these relationships that outputs of (dissimilar) sensors (at different times) can be compared. The residuals resulting from these comparisons are then measures of the discrepancy between the behavior of observed sensor outputs and the behavior that should result under normal conditions. The residual should be zero when the system is normal, and should diverge from zero when a fault occurs in the system. This zero and non-zero property of the residual is used to determine whether or not faults have occurred. Analytical redundancy makes use of a mathematical model and the goal is the determination of faults of a system from the comparison of available system measurements with a priori information

⋆ This material is based upon work supported by the National Science Foundation under Grant No. 0931931 entitled "CPS: Embedded Fault Detection for Low-Cost, Safety-Critical Systems". Any opinions, findings, and conclusions or recommendations expressed in this material are those of the author(s) and do not necessarily reflect the views of the National Science Foundation. This work is supported by the ADDSAFE (Advanced Fault Diagnosis for Safer Flight Guidance and Control) EU FP7 project, Grant Agreement: 233815, Coordinator: Dr. Andrés Marcos. The authors are also thankful for Zoltán Szabó, for providing insight on geometric FDI methods.

represented by the mathematical model, through generation of residual quantities and their analysis. Various approaches have been applied to the residual generation problem, the parity space approach [Chow and Willsky, 1984], the multiple model method [Chang and Athans, 1978], detection filter design using geometric approach [Massoumnia, 1986], frequency domain concepts [Frank, 1990], unknown input observer concept [Chen and Patton, 1999], dynamic inversion based detection [Edelmayer et al., 2003], and using rational nullspace bases [Varga, 2003]. Most of these design approaches refer to linear time-invariant (LTI) systems. The geometric concept is further generalized to linear parameter-varying (LPV) systems by Balas et al. [2003], while input affine nonlinear systems are considered by De Persis et al. [2001]. The basic concepts underlying observer-based fault detection and isolation (FDI) schemes are the generation of residuals and the use of an optimal or adaptive threshold function to differentiate faults from disturbances, see the surveys of Frank [1990], Patton and Chen [1996]. Generally, the residuals, also known as diagnostic signals, are generated by the FDI filter from the available input and output measurements of the monitored system. The threshold function is used to robustify the detection of the fault by minimizing the effects from false faults, disturbances and commands on the residuals. For fault isolation, the generated residual has to include enough information to differentiate said fault from another, usually this is accomplished through structured residuals or directional vectors. Robustness of the FDI algorithm is determined by its capability to decouple the filter performance outputs from disturbances, errors, and unmodelled dynamics. Estimation is important for both signal processing and feedback control and it is the most common approach used in fault detection. The well-known Kalman Filter [Kalman, 1960, Kailath et al., 2000] provides an optimal minimum-variance estimator for linear systems subject to Gaussian noise. The rise of robust control techniques in the 1980s led to an interest in alternative filters, e.g. the $\mathcal{H}_2$ filter (a generalization of the Kalman filter) and the $\mathcal{H}_\infty$ filter ([Shaked and Theodor, 1991]). These methods assume the signals are generated by a known dynamic model and robustness with respect to model uncertainty is an important consideration. Numerous papers on robust filter design have appeared [Appleby et al., 1991, Mangoubi, 1995, Sun and Packard, 2003, Scherer and Köse, 2008].

The geometric design approach, for example, is known for its excellent fault isolation, fault reconstruction and sensitivity properties under small modeling uncertainty and noise. This paper proposes a method incorporate model uncertainty into the design. First, a geometric filter is designed on the nominal plant. Next a robust model matching problem is solved to design a filter that robustly matches the performance of the geometric filter over the set of uncertain plants. It is then shown that the robust model matching problem has an interesting self-optimality property for multiplicative input uncertainty sets. Specifically, the filter designed on the nominal plant is the optimal filter in the robust model matching problem. Finally, an aircraft aileron FDI example is detailed in the present article.

The importance of this paper is on the application (simulation) of the geometric approach based LTI FDI technique to a nonlinear high-fidelity aircraft, where issues of model uncertainty, realistic disturbances and robustness have to be accounted for in the design stage. The remainder of the paper is structured as follows. Section 2 and 3 presents the notation and basic concepts of geometric fault detection filter design. Section 4 formulates the robust fault detection filter design problem and describes the proposed solution method. The application example of a civil aircraft is described in Section 5. The method is applied to the high fidelity aircraft example, which demonstrates the proposed approach, given in Section 6. Finally, the paper is concluded in Section 7.

2. NOTATION

$\mathbb{R}$ and $\mathbb{C}$ denote the set of real and complex numbers, respectively. $\mathbb{RH}_\infty$ denotes the set of proper, rational functions with real coefficients that are analytic in the closed right half of the complex plane. $\mathbb{R}^{m\times n}$, $\mathbb{C}^{m\times n}$, and $\mathbb{RH}_\infty^{m\times n}$ denote the sets of $m\times n$ matrices whose elements are in $\mathbb{R}$, $\mathbb{C}$, and $\mathbb{RH}_\infty$, respectively. A single superscript index is used to denote vectors, e.g. $\mathbb{R}^l$ denotes the set of $l\times 1$ vectors whose elements are in $\mathbb{R}$. For a matrix $M\in\mathbb{C}^{m\times n}$, M^* denotes the complex conjugate transpose. $\bar\sigma(M)$ and $\underline\sigma(M)$ denote the maximum and minimum singular values. $\|M\|$ denotes the matrix norm induced by the vector 2-norm. It is known that $\|M\|=\bar\sigma(M)$. For a vector $v\in\mathbb{C}^n$, $Re[v]$ denotes the real part of v. For $G\in\mathbb{RH}_\infty^{m\times n}$, $\|G\|_\infty := \sup_\omega \bar\sigma(G(j\omega))$. Finally, let $G\in\mathbb{RH}_\infty^{(n+k)\times(n+m)}$ and $\Delta\in\mathbb{RH}_\infty^{n\times n}$ be given and partition $G := \left[\begin{smallmatrix} G_{11} & G_{12}\\ G_{21} & G_{22}\end{smallmatrix}\right]$ with $G_{11}\in\mathbb{RH}_\infty^{n\times n}$ and $G_{22}\in\mathbb{RH}_\infty^{k\times m}$. If $I-G_{11}\Delta$ is invertible at $\omega=\infty$, then define $F_u(G,\Delta)$ as the linear fractional transformation (LFT) obtained by closing Δ around the upper channels of G:

$$F_u(G,\Delta) := G_{22} + G_{21}\Delta\left(I-G_{11}\Delta\right)^{-1}G_{12} \qquad (1)$$

3. GEOMETRIC FDI FILTERS

This section briefly describes the formulation of fault detection filters designed using geometric concepts. The derivation of the geometric FDI filters is presented for LTI systems with no disturbance, no uncertainty and the detection and isolation of two faults. Consider the LTI system with two additive actuator faults:

$$\begin{aligned}\dot x(t) &= Ax(t)+Bu(t)+L_1f_1(t)+L_2f_2(t)\\ y(t) &= Cx(t)\end{aligned} \qquad (2)$$

where L_1 and L_2 represent the faults directions in the state space. f_1 and f_2 are the fault signals. The fault signals are zero if there is no fault but nonzero if the particular fault occurs. Only actuator faults are considered here but sensor faults can also be considered within the theory. The fundamental problem of residual generation is to synthesize residual generators (filters) with outputs r_i $(i=1,2)$ that have the following decoupling property: r_i is sensitive to f_i but insensitive to f_j, $i\neq j$. More precisely, if $f_i=0$ then $\lim_{t\to\infty} r_i(t)=0$ and if $f_i\neq 0$ then $r_i\neq 0$.

The solution of this problem depends on the (C,A)-invariant subspaces and certain unobservability subspaces [Massoumnia, 1986]. A (C,A)-unobservability subspace $\mathcal{S}$

is a subspace such that there exist matrices G and H with the property that $\mathcal{S}$ is the maximal $(A + GC)$ invariant subspace contained in Ker HC. The family of (C, A)-unobservability subspaces containing a given set $\mathcal{L}$ has a minimal element. Define $\mathcal{L}_i = \text{Im } L_i$ $(i = 1, 2)$ and denote by $\mathcal{S}^*$ the smallest unobservability subspace containing $\mathcal{L}_2$. Then the fundamental problem of residual generation has a solution if and only if $\mathcal{S}^* \cap \mathcal{L}_1 = 0$ [Massoumnia et al., 1989]. The condition $\mathcal{S}^* \cap \mathcal{L}_1 = 0$ ensures that the fault to be detected is not hidden in the unobservability subspace of the detection filter. In fact, the fault direction will be decoupled from the rest of the fault directions since they are contained in the unobservability subspace of the residual generator. This result can be extended to LPV systems [Balas et al., 2003] and to nonlinear input affine systems [De Persis et al., 2001].

The residual generator associated with fault direction L_1 can be described by an observer of the form:

$$\begin{aligned} \dot{w}(t) &= Nw(t) - Gy(t) + Fu(t) \\ r_1(t) &= Mw(t) - Hy(t) \end{aligned} \tag{3}$$

where u and y are the known input and measured output signals of the original LTI system. w is the state of the residual generator and r_1 is the residual.

Denote by P the projection operator $P : \mathcal{X} \to \mathcal{X}/\mathcal{S}^*$. The state matrices can be determined as follows [Massoumnia, 1986]. H is a solution of the equation Ker $HC =$ Ker $C +$ $\mathcal{S}^*$, and M is the unique solution of $MP = HC$. Consider a gain matrix $\hat{G}$ chosen such that $(A + \hat{G}C)\mathcal{S}^* \subseteq \mathcal{S}^*$ and define $\hat{A} = P(A+GC)P^T$. $\hat{A}$ is not necessarily Hurwitz. To obtain quadratically stable filters one can set $N = \hat{A}+\tilde{G}M$, where $\tilde{G} := X^{-1}K$ and X, K are determined from the linear matrix inequality (LMI):

$$0 \succeq \hat{A}^T X + X\hat{A} + M^T K^T + KM \tag{4}$$

$$0 \preceq X = X^T \tag{5}$$

Then set $G = P\hat{G} + \tilde{G}H$ and $F = PB$.

Using this approach there are as many filters as faults to detect, and their state dimensions are equal to the dimension of $\mathcal{X}/\mathcal{S}^*$. The filter poles can be tuned by imposing constraints in the LMI resulting in perfect reconstruction of fault signals f_i. One issue is that the filter design does not consider model uncertainty and the fault detection performance may be not be robust. The next section discusses a model matching approach for recovering the geometric filter performance in the presence of model uncertainty.

4. ROBUST MODEL MATCHING

This section considers a robust model matching problem for geometric filter design on uncertain plants. Then several existing methods for robust filter synthesis are described. The final subsection shows that the robust model matching problem has an interesting self-optimality property for multiplicative input uncertainty sets.

4.1 Problem Formulation

Let G_u denote an uncertain plant for which the filter will be designed. The standard linear fractional transformation (LFT) framework [Packard and Doyle, 1993, Zhou et al., 1996] can be used to model the uncertainties. Let $G \in \mathbb{RH}_\infty^{(n+k)\times(n+m)}$ and $\mathbf{\Delta} \subseteq \mathbb{RH}_\infty^{n\times n}$ be given.[1] Define the set of models

$$\mathcal{M} := \{G_u = F_u(G, \Delta) : \Delta \in \mathbf{\Delta},\ \|\Delta\|_\infty \leq 1\} \tag{6}$$

It is assumed that $F_u(G, \Delta)$ is well defined for all $\Delta \in \mathbf{\Delta}$ with $\|\Delta\|_\infty \leq 1$. $\mathbf{\Delta}$ is typically a set describing a block structured system that can include (repeated) real parametric and LTI dynamic system uncertainties. Nonlinear and/or time-varying uncertainties can also be modeled using integral quadratic constraints [Megretski and Rantzer, 1997]. The restriction that Δ be a square system is only for notational simplicity.

Each $G_u \in \mathcal{M}$ is a system that relates the faults and plant inputs to the signals available to the fault detection filter:

$$\begin{bmatrix} y \\ u \end{bmatrix} = G_u \begin{bmatrix} f \\ u \end{bmatrix} \tag{7}$$

The objective is to design a filter F with inputs $\left[\begin{smallmatrix} y \\ u \end{smallmatrix}\right]$ and output residuals r such that the residuals have "good" fault decoupling properties for all models $G_u \in \mathcal{M}$.

A robust model matching problem is now described to meet this objective. The nominal plant in the set $\mathcal{M}$ is given by $\Delta = 0$, i.e. $G_0 := F_u(G, 0)$ is the nominal plant. First, design a geometric filter F_0 to solve the fundamental problem of residual generation on the nominal plant G_0. The model matching method attempts to design a filter F such that the performance on the uncertain plant G_u robustly matches the designed behavior of F_0G_0. Mathematically, the proposed design problem is:

Problem 1. Let $G \in \mathbb{RH}_\infty^{(n+k)\times(n+m)}$, $\mathbf{\Delta} \subseteq \mathbb{RH}_\infty^{n\times n}$ and $F_0 \in \mathbb{RH}_\infty^{l\times k}$ be given. The *robust model matching problem* is:

$$\min_{F\in\mathbb{RH}_\infty^{l\times k}} \max_{G_u\in\mathcal{M}} \|F_0G_0 - FG_u\|_\infty \tag{8}$$

The interconnection for this robust model matching problem is shown in shown in Figure 1. The reference model is given by F_0G_0. The nominal residual response r_0 will have the desired decoupling properties given by the fundamental problem of residual generation. The optimization in Equation 8 designs a filter F that most closely matches, in a worst-case sense, the desired residual generation behavior F_0G_0. In this paper the focus is on fault detection filters designed using the geometric approach but the model matching problem can, in principle, be used to robustly match the behavior of any filter F_0 designed on the nominal system G_0.

4.2 Filter Synthesis

There are several approaches to solve the robust model matching problem. Sun and Packard observed that robust filter design (Equation 8) is an infinite-dimensional convex optimization in the filter [Sun and Packard, 2003]. They developed an algorithm to compute the globally optimal robust filter for the special case where $\mathbf{\Delta}$ only models

[1] G and F were used in the previous section to denote gain matrices in the geometric filter. In this section G and F will denote systems in the model matching design.

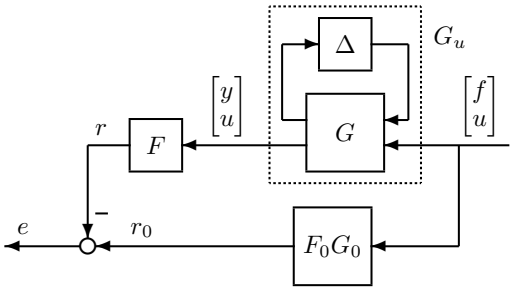

Fig. 1. Robust model matching.

repeated real uncertainties. It does not seem possible to extend this algorithm to sets $\mathbf{\Delta}$ that include dynamic uncertainties, nonlinearities and/or time-varying operators.

The standard approach to handle more complicated uncertainty sets is to replace $\max_{G_u \in \mathcal{M}} \|F_0G_0 - FG_u\|_\infty$ with an upper-bound. For example, when $\mathbf{\Delta}$ contains only LTI uncertainty the maximization over $\mathcal{M}$ can be replaced with the μ upper bound which involves a minimization over D scales [Dullerud and Paganini, 2000]. The design problem can then be recast as a μ-synthesis problem involving a search for the filter and the D scales. μ-synthesis is, in general, a nonconvex problem and the coordinate-wise D-K iteration has been applied to solve for the filter and uncertainty multipliers [Appleby et al., 1991]. The D-K iteration yields sub-optimal solutions but is a standard method to handle the nonconvexity that arises in robust control synthesis.

In robust filter design problem, the filter enters the design interconnection in an open loop (rather than a feedback) configuration and this structure can be exploited. There are two different approaches to convert the μ-synthesis problem into an infinite dimensional convex optimization problem ([Scherer and Köse, 2008] and [Seiler et al., 2011]). Both approaches use the more general IQC framework to model the uncertainty and obtain an upper bound on the worst-case performance. In [Scherer and Köse, 2008], the filter synthesis problem is converted into an infinite-dimensional (convex) semi-definite program (SDP) [Boyd et al., 1994]. The set of allowable IQC multipliers is infinite dimensional and a finite dimensional optimization is obtained by restricting the multipliers to be a combination of chosen basis functions. In [Seiler et al., 2011], the robust filter design problem is turned into a frequency-dependent, infinite dimensional linear matrix inequality (LMI) in the filter and multipliers. Next, a finite dimensional optimization is obtained by enforcing the frequency-dependent LMI on a dense frequency grid and restricting the filter to be a linear combination of chosen basis functions. The frequency-dependent IQC multipliers are allowed to be arbitrary functions on the frequency grid. To summarize, the two approaches use roughly dual methods to convert the robust filter design problem to a finite dimensional convex optimization: In [Seiler et al., 2011], basis functions are used for the filter but the multipliers (scalings) are allowed to be arbitrary functions on the frequency grid. In [Scherer and Köse, 2008] basis functions are chosen for the multipliers but the filter is allowed to be an arbitrary, linear system.

The various methods to solve the robust filter design problem have benefits and drawbacks in terms of computational complexity and ease of formulating the problem (e.g. picking basis functions for the filter or for the uncertainty scalings). The next section shows that the robust model matching problem has an interesting self-optimality property for multiplicative input uncertainty sets. Specifically, F_0 itself is the optimal filter for this uncertainty structure.

4.3 Multiplicative Input Uncertainty

This section considers the robust model matching problem for input multiplicative uncertainty. The uncertain system is given by $G_u := G_0(I + w\Delta)$ where $w \in \mathbb{RH}_\infty$ is a weight that specifies the level of uncertainty at each frequency by $|w(j\omega)|$. $|w(j\omega)| = 1$ corresponds to 100% input uncertainty at frequency ω and hence weights typically satisfy $\|w\|_\infty \leq 1$. Input multiplicative uncertainty is a commonly used uncertainty model because the effect of uncertainty can be quickly assessed by choosing simple weights w. For example, a reasonable uncertainty model is obtained by choosing w to be a first order system with small magnitude at low frequencies and magnitude close to one at high frequencies. Alternatively, the Matlab function `ucover` [Balas et al., 2010] can be used to compute a w so that the uncertainty set $\mathcal{M}$ contains a given, finite set of LTI systems. The weight can generally be chosen as a full matrix but the result in this section is restricted to weights of the form $w(s)I$.

The design interconnection for the robust model matching problem with input multiplicative uncertainty is shown in Figure 2. G_0 again denotes the nominal system and F_0 is a filter that has been designed to achieve some desired performance on the nominal plant. For this uncertainty structure the robust model matching problem can be equivalently stated as:

Problem 2. Let $F_0 \in \mathbb{RH}_\infty^{m\times n}$, $G \in \mathbb{RH}_\infty^{n\times k}$ and $w \in \mathbb{RH}_\infty$ be given. The *robust model matching problem* is:

$$\min_{F\in\mathbb{RH}_\infty^{m\times n}} \max_{\Delta\in\mathbb{RH}_\infty^{k\times k}, \|\Delta\|_\infty\leq 1} \|F_0G - FG(I + w\Delta)\|_\infty \quad (9)$$

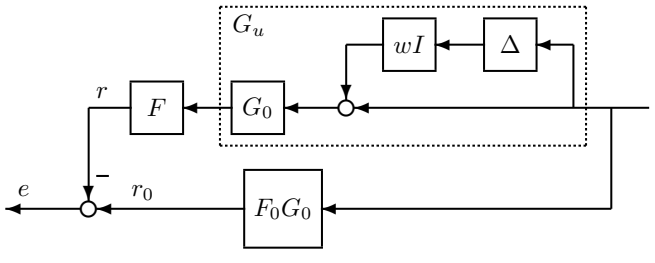

Fig. 2. Robust model matching with multiplicative input uncertainty.

The next theorem presents the main result of this section.

Theorem 3. If $\|w\|_\infty \leq 1$ then F_0 is the optimal filter for the robust model matching problem.

Proof 1. The robust model matching problem can be equivalently written as:

$$\min_{F\in\mathbb{RH}_\infty^{m\times n}} \max_{\omega} \max_{\substack{\Delta\in\mathbb{RH}_\infty^{k\times k} \\ |\Delta(j\omega)|\leq|w(j\omega)|}} \|\left(F_0G - FG(I + \Delta)\right)(j\omega)\|$$

The min-max is always greater than the max-min and hence a lower bound on the model matching problem is obtained by:

$$\max_{\omega} \min_{F \in \mathbb{RH}_{\infty}^{m \times n}} \max_{\substack{\Delta \in \mathbb{RH}_{\infty}^{k \times k} \\ |\Delta(j\omega)| \leq |w(j\omega)|}} \| \left(F_0 G - FG(I+\Delta)\right)(j\omega) \| \tag{10}$$

Next, the constraints that F and Δ be stable are dropped:

$$\max_{\omega} \left[\min_{F \in \mathbb{C}^{m \times n}} \max_{\substack{\Delta \in \mathbb{C}^{k \times k} \\ |\Delta| \leq |w(j\omega)|}} \|(F_0 G)(j\omega) - FG(j\omega)(I+\Delta)\| \right] \tag{11}$$

The max over Δ is unchanged by dropping the stability constraint but the min over F is potentially lower once we drop the stability constraint. Thus the result of Equation 11 is no greater than the optimal value for Equation 10.

Next, apply Lemma 5 in the appendix with $A := F_0(j\omega)$, $B := G(j\omega)$, and $\alpha := |w(j\omega)|$. By this lemma and the assumption $\|w\|_{\infty} \leq 1$, the optimization in the brackets of Equation 11 has an optimal cost equal to $|w(j\omega)| \|(F_0 G)(j\omega)\|$ at each ω and the optimal value is achieved by $F = F_0(j\omega)$.

Thus the optimal cost for the robust model matching problem is lower bounded by $\|wF_0G\|_{\infty}$. This cost is achieved by the choice $F = F_0$ and hence F_0 is the optimal filter.

Roughly, this result implies that the robust model matching filter design is self optimal for this input multiplicative uncertainty set. The uncertainty degrades the performance but it does so in a way that apparently cannot be exploited by any other filter. Note that this result is not specific to nominal filters F_0 designed with the geometric method. The result only depends on the formulation of the robust model matching problem and the specific structure of the input multiplicative uncertainty.

5. AIRCRAFT MODEL

5.1 General Aircraft Characteristics

The aircraft model used in this paper is an aircraft from Airbus. The aircraft has two engines and a nominal weight of 200 tons. Some of its performance at cruise flight condition are speed of 240 knots, altitude of 30000 ft. The aircraft has 19 control inputs, and measurement of 6-DOF motion with load factor (n_x, n_y, n_z), body rate (p, q, r), velocity (V_T), aerodynamic angles (α, β), position (X, Y, Z) and attitude (ϕ, θ, ψ) outputs. The inputs are: $pi1$ left and $pi2$ right engine; AF (airbrake), which is disabled at cruise flight condition, $\delta_{a,IL}$ Aileron internal Left; $\delta_{a,IR}$ Aileron internal Right; $\delta_{a,EL}$ Ail external Left; $\delta_{a,ER}$ Ail external Right; $\delta_{sp,1L}$ Spoiler 1 Left; $\delta_{sp,1R}$ Spoiler 1R; Spoiler 23L; Spoiler 23R; Spoiler 45L; Spoiler 45R; $\delta_{sp,6L}$ Spoiler 6L; $\delta_{sp,6R}$ Spoiler 6R; $\delta_{e,L}$ Elevator Left; $\delta_{e,R}$ Elevator Right; δ_r Rudder; and δ_{ih} Trimmable Horizontal Stabilizer which is used for trimming purposes.

The aerodynamic database, propriety of Airbus Operations S.A.S, is of high-fidelity. The rigid body aircraft equations of motion are augmented with actuator [Goupil, 2009b] and sensor characteristics. The nonlinear body-axes rigid body dynamics includes 13 states using quaternion formalism: p, q, r body rates, u, v, w velocities all in body axes, q_0, q_1, q_2, q_3 quaternions, representing the rotation between the body and inertial axes, and X, Y, Z positions in the North-East-Down coordinate frame, assuming Flat Earth for simplicity.

5.2 Linearized Aircraft Model

In the present article one design point, cruise flight condition, is considered. The LTI model of the aircraft is obtained at level flight, with $p = q = r = 0$ rad/s, $v_x = 194.36$ m/s, $v_y = 0m/s$, $v_z = 15.13$ m/s, at 9144 m altitude, see Vanek et al. [2011] for details. The airbrake, which is disabled at high Mach numbers, is removed from the control inputs since it has no effect on the aircraft. Since the original aircraft model uses quaternions, which impose additional constraints on the state equations, the model used for trim and linearization is rewritten using conventional Euler angles [Stengel, 2004]. The model used for trim is an open-loop model without the control loop and, since the actuators and sensors are assumed to have unit steady state gain and low-pass characteristics, their dynamics are omitted. Trim is obtained with zero aileron, rudder and elevator deflection, left and right engines are providing the same amount of thrust to balance the yawing motion. Pitch axis trim is obtained with the Trimmable Horizontal Stabilizer, while the aircraft has 2.66 degrees Angle-of-attack. The resulting 12 state linear model is unstable.

The open loop aircraft model is slightly unstable around the yaw angle (ψ), and has two modes (X, Y) which are integrators. Since the FDI problem is invariant of X, Y positions and yaw angle these states are removed from the dynamics. The resulting model with nine states, as described in [Vanek et al., 2011], almost perfectly matches the original 12 states model in the behavior of the remaining states, and outputs. The resulting system with nine states is stable which is necessary for linear estimator based FDI techniques.

The resulting LTI model can be augmented with first order sensor and actuator dynamics derived from the high-fidelity simulation, to account for their effect on the aircraft behavior. Since the filters obtained by geometrical FDI methods require intense computation onboard the aircraft, only the pure rigid body dynamics model is used for filter synthesis here.

6. FDI FILTER DESIGN FOR THE AIRCRAFT

A geometric LTI FDI filter is designed for the aileron fault detection problem of the aircraft. First, the filter design steps are detailed and supported by linear analysis plots to show the optimality of the geometric filter. Detailed simulations on the high-fidelity aircraft model with injected aileron faults follows.

6.1 Filter Design Steps

The main idea behind the filter design formulation is that aileron faults appear on the filter residual output,

while elevator and rudder faults are embedded in the unobservability subspace of the filter. For that reason the LTI model derived in Section 5.2 is augmented with left inner aileron, left elevator, and rudder faults, by using the successive input directions from the B and D matrices as fault directions in the linear model. Load factor, n_x, n_y, and n_z, measurement is omitted from the model, since the D matrix associated with these acceleration outputs is nonzero, which makes the geometric FDI synthesis more complicated. The resulting filter, using the methods developed in [Massoumnia, 1986], has 1 residual output, 27 inputs, and 7 states. Since perfect decoupling is possible, the transfer functions between elevator to residual and rudder to residual are zero, while the residual have $0.394 rad/s$ time constant tracking response for aileron faults.

A lower bound on the optimal performance is computed using frequency-gridding method described in [Seiler et al., 2011], when the system is exposed to uncertainty. In the nominal case, with no uncertainty, the geometric filter is optimal for the decoupling, and according to Theorem 3 the filter is also optimal when input multiplicative uncertainty is considered. The effect of structured, input multiplicative uncertainty with the weights of $w_1 = \frac{2s+2}{s+60}$ on engines,$w_2 = \frac{2s+8}{1160}$ on spoilers, $w_3 = \frac{1.5s+3}{1120}$ on ailerons, elevators, and rudders , and $w_4 = \frac{14}{1160}$ on trimmable horizontal stabilizers are considered, with time constants comparable with the different actuator bandwidths. These weights corresponds to more than 100% uncertainty at high frequencies and 5% uncertainty at low frequencies on the input channels, and the block structure of the uncertainty Δ_a is grouped according to the actuator functional groups: $\Delta_a = diag < \Delta^{2\times2}_{engine}, \Delta^{4\times4}_{aileron}, \Delta^{8\times8}_{spoiler}, \Delta^{3\times3}_{longitudinal}, \Delta^{1\times1}_{rudder} >$.

The frequency grid consisted of 50 logarithmical spaced points between 0.01 and $100 rad/sec$. Figure 3 shows the lower bounds versus frequency. The dashed curve in Figure 3 shows the worst-case performance of F_0. The performance of F_0 degrades by approximately 41% over the uncertainty set, from perfect decoupling corresponding to 0 lower bound of the nominal case. The solid curve in Figure 3 shows the lower bound on the best achievable filter performance with uncertainty set included. The two curves are equal as expected based on Theorem 3. Thus F_0 is the optimal filter for robustly matching its own performance on the nominal plant. To further investigate the performance of the obtained filter, the uncertain LTI aircraft model is augmented with first order sensor and actuator models, on all input and output channels. Since the corresponding mathematical models are Airbus propriety, they are not discusses here. A lower bound calculation indicates in Figure 4 that the achievable performance is not significantly higher, compared with the actuator- and sensorless case, but the performance of the nominal filter is significantly lower than the achievable minimum. Due to these results, it is desirable to have actuator and sensor dynamics included in the filter design, which is not the case here since computational complexity of those filters are significantly higher.

The filters are applied to the nonlinear aircraft model after taking the trim values into consideration, on both control input and sensor output signals. Since the simulation

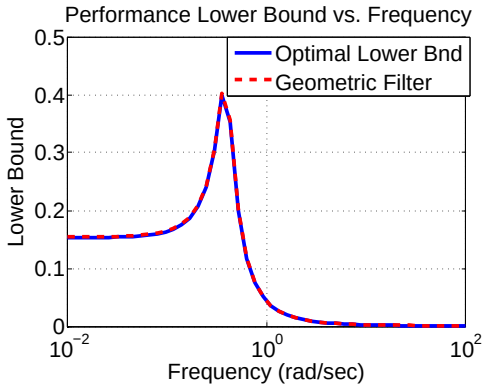

Fig. 3. Theoretical lower bound and achieved lower bounds of the FDI problem formulation with input multiplicative uncertainty.

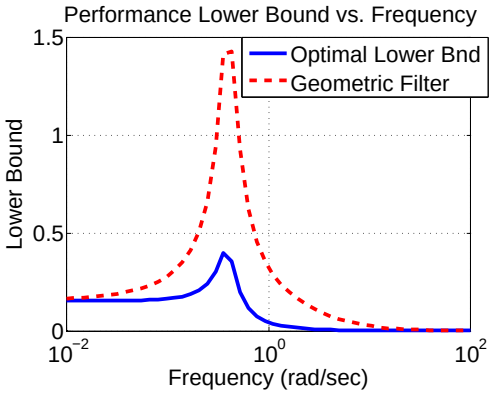

Fig. 4. Theoretical, and achieved lower bounds of the FDI problem formulation with input multiplicative uncertainty, augmented actuator and sensor models.

is implemented under SIMULINK with $0.01 sec$ fixed step size, the corresponding filters are also discretized with the same sampling time using bilinear transformation. It is also worth mentioning, that the simulation is in closed-loop with the flight control system set to altitude and heading hold mode and moderate atmospheric windgust disturbances are perturbing the aircraft flight.

The first fault scenario is left inboard aileron liquid jamming as seen on Figure 5, this means that a bias occurs on the rod sensor and the actuator shifts from it nominal $1.5 deg$ deflection to $-0.75 deg$ deflection and it remains $-2.25 deg$ apart from it commanded position. Figure 5 also shows the abrupt change in roll rate at $25 sec$ when the fault occurs, otherwise slight deflection can be seen on the rudder but elevator and THS is unaffected, mainly the right aileron compensates the effect of the failure.

After investigation of fault free flight profiles, a detection threshold of 0.125 is selected. This corresponds to 100% margin over the largest observed residual signal with no fault. It is worth to note, that significantly lower detection threshold is achievable when the atmospheric windgust disturbances have lower level. Using the above mentioned threshold a detection time of 3.12 seconds is achieved, as shown on Figure 6, which is satisfactory since the level of

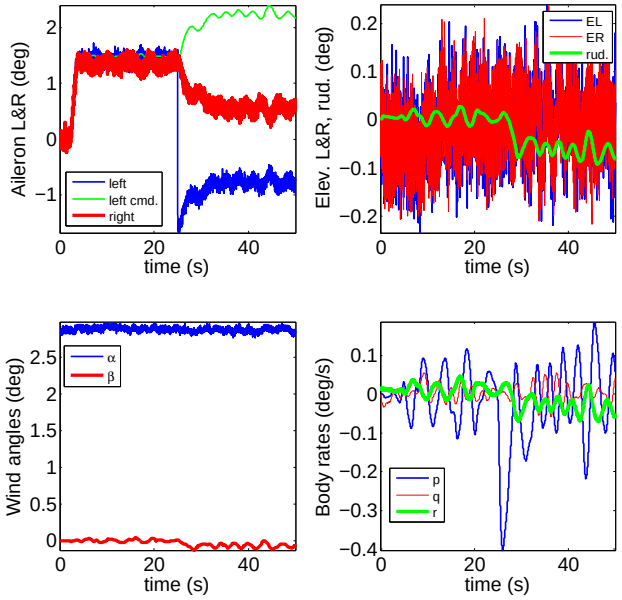

Fig. 5. Left aileron liquid jamming scenario, fault occurs at $25s$.

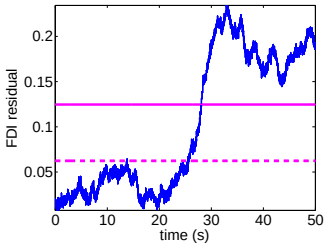

Fig. 6. Aileron liquid jamming, geometric FDI filter residual.

fault only affects optimal aircraft configuration and is not critical to be detected instantaneously.

The second fault scenario is left inboard aileron disconnection as seen on Figure 7, this occurs when the connection between the actuator rod and the control surface is lost due to mechanical separation of the two components. Due to the aerodynamic forces, the freely floating aileron goes to -12 deg where it is reaching its physical limit, while the commanded position still remains positive as seen on Figure 7. The large unintended deflection leads to significant deviation from trim condition and the flight controller tries to compensate against it mainly in the lateral channel with rudder and right aileron, while the elevator commands are not influenced (see Fig.7). Significant sideslip can be seen also, which is due to asymmetric aircraft configuration, while roll rate has almost 2.5 deg/s peak after the fault occurs.

Since this fault creates large roll rate and sideslip motion, which also leads to significant structural stress in the wings the detection of this fault is critical. Figure 8 shows a detection time of 1.26 seconds, which is lower than the detection of the jamming but it is desired to have shorter detection times in industrial implementation, to be able to detect such failures before large wind deformation is present.

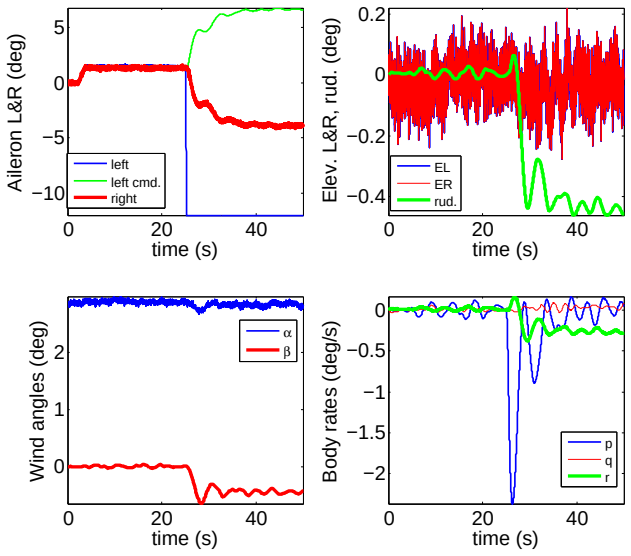

Fig. 7. Left aileron disconnection scenario, fault occurs at $25s$.

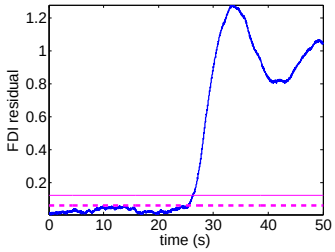

Fig. 8. Left aileron disconnection, geometric FDI filter residual.

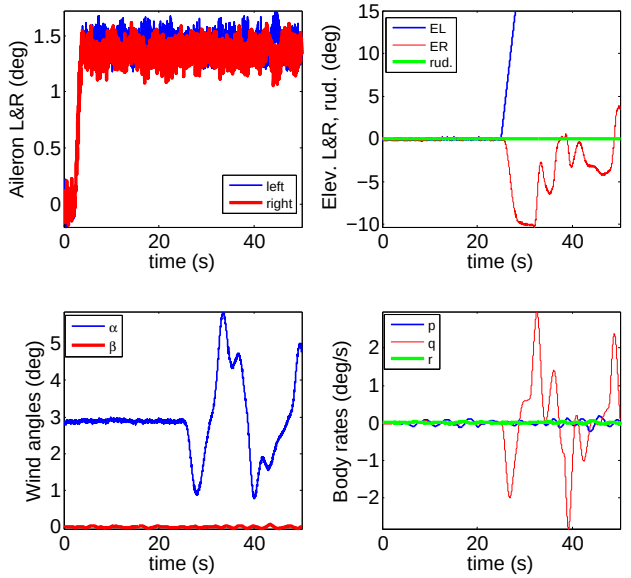

Fig. 9. Left elevator runaway scenario, fault occurs at $25s$.

To be able to asses the decoupling performance of the FDI filter for other types of faults a left elevator runaway scenario is also investigated as shown in Figure 9. The left elevator starts to drift from its commanded position with 5 deg/s rate.

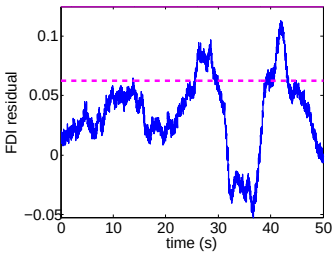

Fig. 10. Left elevator runaway, geometric (aileron) FDI filter residual.

As seen on Figure 9 the fault creates significant pitch rate response and the angle of attack also changes dramatically during the maneuver, which leads to covering large part of the flight envelope. The right elevator with lower response time and later the THS compensates against the failure effect.

As seen on Figure 10, the residual signal increases, due to deviation from the trim flight condition, where the linear model used in the FDI filter design is no more accurate. But the residual signal stays away from the detection threshold and as soon as the aircraft motion is stabilized the residual goes back to near zero value.

7. CONCLUSIONS

This paper considers the design of geometric fault detection filters and their application to a high fidelity aircraft model, and shows the advantages of advanced model-based methods, those are candidates for future industrial implementation. First, a geometric filter is designed on the nominal plant. Next a robust model matching problem is solved to design a filter that robustly matches the performance of the geometric filter over the set of uncertain plants. It is then shown that the robust model matching problem has an interesting self-optimality property for multiplicative input uncertainty sets. The proposed LTI filter is then applied to a high-fidelity aircraft model, where different aileron faults are successfully detected and when designed properly isolated from elevator and rudder faults in reasonable time. Further research should extend the validity of the present approach and based on the present findings provide a fault detection approach for a larger flight envelope.

REFERENCES

B. Appleby, J. Dowdle, and W. VanderVelde. Robust estimator design using μ synthesis. In *Proc. of the IEEE Conference on Decision and Control*, pages 640–645, 1991.

G. Balas, J. Bokor, and Z. Szabo. Invariant subspaces for LPV systems and their applications. *IEEE Transactions on Automatic Control*, 48(11):2065–2069, 2003.

G. Balas, R. Chiang, A. Packard, and M. Safonov. *Robust Control Toolbox*. MathWorks, 2010.

S. Boyd, L. El Ghaoui, E. Feron, and V. Balakrishnan. *Linear Matrix Inequalities in System and Control Theory*, volume 15 of *Studies in Applied Mathematics*. SIAM, 1994.

C. B. Chang and M. Athans. State estimation for discrete systems with switching parameters. *IEEE Transactions on Aerospace and Electronic Systems*, 14:418–425, 1978.

J. Chen and R. J. Patton. *Robust Model-based Fault Diagnosis for Dynamic Systems*. Kluwer Academic. Boston., 1999.

E.Y. Chow and A.S. Willsky. Analytical redundancy and the design of robust failure detection systems. *IEEE Trans. on Automatic Control*, 29(7):603–614, 1984.

C. De Persis, R. De Santis, and A. Isidori. Nonlinear actuator fault detection and isolation for a VTOL aircraft. In *Proceedings of the 2001 American Control Conference, Vols 1-6*, pages 4449–4454, 2001.

G. Dullerud and F. Paganini. *A course in robust control theory: A convex approach*. Springer Verlag, 2000.

A. Edelmayer, J. Bokor, and Z. Szabo. A geometric view on inversion-based detection filter design in nonlinear systems. In *Proceedings of the 5th IFAC symposium on fault detection, supervision and safety of technical processes. SAFEPROCESS 2003, Washington*, pages 783–788, Washington, 2003.

P.M Frank. Fault diagnosis in dynamic systems using analytical and knowledge-based redundancy - a survey and some new results. *Automatica*, 26:459–474, 1990.

P. Goupil. Airbus state of the art and practices on fdi and ftc. In *Proceedings of Safeprocess'09*, 2009a.

Philippe Goupil. Oscillatory failure case detection in the a380 electrical flight control system by analytical redundancy. *Control Engineering Practice*, 18:1110–1119, 2009b.

T. Kailath, A.H. Sayed, and B. Hassibi. *Linear Estimation*. Prentice-Hall, 2000.

R.E. Kalman. A new approach to linear filtering and prediction problems. *Trans. ASME, Ser D., Journal of Basic Engineering*, 82:35–45, 1960.

R.S. Mangoubi. *Robust Estimation and Failure Detection For Linear Systems*. PhD thesis, Massachusetts Institute of Technology, 1995.

M.A. Massoumnia. A geometric approach to the synthesys of failure detection filters. *IEEE Transactions on Automatic Control*, 31:839–846, 1986.

M.A. Massoumnia, G.C. Verghese, and A.S. Willsky. Failure detection and identification. *IEEE Transactions on Automatic Control*, 34:316–321, 1989.

A. Megretski and A. Rantzer. System analysis via integral quadratic constraints. *IEEE Trans. on Automatic Control*, 42(6):819–830, 1997.

A. Packard and J. Doyle. The complex structured singular value. *Automatica*, 29(1):71–109, 1993.

R. J. Patton and J. Chen. Robust fault detection and isolation FDI systems. *Contr. Dynamic Syst.*, 74:176–224, 1996.

C.W. Scherer and I.E. Köse. Robustness with dynamic IQCs: An exact state-space characterization of nominal stability with applications to robust estimation. *Automatica*, 44:1666–1675, 2008.

P. Seiler, B. Vanek, J. Bokor, and G.J. Balas. Robust H_∞ filter design using frequency gridding. In *Submitted to the 2011 American Control Conference*, 2011.

U. Shaked and Y. Theodor. H_∞-optimal estimation: A tutorial. In *Proc. of the IEEE Conference on Decision and Control*, pages 2278–2286, 1991.

Robert F. Stengel. *Flight Dynamics*. Princeton University Press, 2004.

K. Sun and A. Packard. Optimal, worst-case filter design via convex optimization. In *Proc. of the IEEE Confer-*

ence on Decision and Control, pages 1380–1385, 2003.

D. Van den Bossche. The a380 flight control electrohydrostatic actuators, achievements and lessons learnt. In *Proc. 25th Congress of the International Council of the Aeronautical Sciences*, 2006.

B. Vanek, P. Seiler, J. Bokor, and G.J. Balas. Robust fault detection filter design for commercial aircraft. In *Euro GNC 2011 1st CEAS Specialist Conference on Guidance, Navigation & Control, Münich*, 2011.

A. Varga. On computing least order fault detectors using rational nullspace bases. In *In Proceedings of the IFAC Symp. SAFEPROCESS'2003, Washington D.C.*, 2003.

Kemin Zhou, J.C. Doyle, and K. Glover. *Robust and Optimal Control*. Prentice-Hall, 1996.

Appendix A

Lemma 4. Let $c_1, c_2 \in \mathbb{R}$ be non-negative constants. If $u, v \in \mathbb{C}^n$ and $Re[u^*v] \geq 0$ then $\|c_1 u\| \leq \|c_1 u + c_2 v\|$.

Lemma 5. Let $\alpha \in \mathbb{R}$ be a strictly positive constant and let $A \in \mathbb{C}^{m\times n}$ and $B \in \mathbb{C}^{n\times k}$ be given matrices. Define $J : \mathbb{C}^{m\times n} \to \mathbb{R}$ as:

$$J(X) := \max_{\Delta\in\mathbb{C}^{k\times k}, \bar{\sigma}(\Delta)\leq\alpha} \|AB - XB - XB\Delta\| \qquad \text{(A.1)}$$

Then

$$\min_{X\in\mathbb{C}} J(X) = \begin{cases} \alpha\|AB\| & \text{if } \alpha \leq 1 \\ \|AB\| & \text{if } \alpha > 1 \end{cases} \qquad \text{(A.2)}$$

The minimal cost is achieved by $X^* = A$ if $\alpha \leq 1$ and $X^* = 0$ if $\alpha > 1$.

Proof 2. Let $u \in \mathbb{C}^k$ and $v \in \mathbb{C}^m$ be the input/output vectors associated with the maximum singular value of AB, i.e. u and v satisfy $ABu = \bar{\sigma}(AB)v$, $\|u\| = 1$, and $\|v\| = 1$.

Assume $\alpha > 1$ and pick any $X \in \mathbb{C}^{m\times n}$. If $Re[(XBu)^*v] \geq 0$ then choose $\Delta_0 = -\alpha I$. $J(X)$ can be lower-bounded as:

$$\begin{aligned} J(X) &\geq \|AB - XB - XB\Delta_0\| \\ &= \|AB + (\alpha - 1)XB\| \\ &\geq \|\left(AB + (\alpha - 1)XB\right)u\| \\ &\geq \|\bar{\sigma}(AB)v + (\alpha - 1)XBu\| \\ &\geq \bar{\sigma}(AB) \end{aligned}$$

The first inequality follows from the definition of $J(X)$ in Equation A.1 while the equality follows from the definition of Δ_0. The next two inequalities follow from the definition of the matrix norm (maximum singular value) and the choices of u and v. The final inequality follows from Lemma 4. If $Re[(XBu)^*v] \leq 0$ then similar steps can be used to again show that $J(X) \geq \bar{\sigma}(AB)$ with the choice $\Delta_0 = +\alpha I$. Thus $J(X) \geq \bar{\sigma}(AB)$ and the lower bound is achieved by $X = 0$.

Next assume $\alpha \leq 1$. Pick any $X \in \mathbb{C}^{m\times n}$ and define $Y := -A + X$. If $Re[(YBu)^*v] \geq 0$ then choose $\Delta_0 = \alpha I$. Similar to the steps above, $J(X)$ can be lower-bounded as:

$$\begin{aligned} J(X) &\geq \|\alpha AB + (\alpha + 1)YB\| \\ &\geq \|\alpha\bar{\sigma}(AB)v + (\alpha + 1)YBu\| \\ &\geq \alpha\bar{\sigma}(AB) \end{aligned}$$

The first inequality follows from the choice of Δ_0 and the definition of Y. The next inequality again follow from the choices of u and v while the final inequality follows from Lemma 4. If $Re[(YBu)^*v] \leq 0$ then similar steps can be used to show that $J(X) \geq \alpha\bar{\sigma}(AB)$ with the choice $\Delta_0 = -\alpha I$. Thus $J(X) \geq \alpha\bar{\sigma}(AB)$ and the lower bound is achieved by $X = A$.